An analysis of $h \to \mu^+\mu^-$ mode at the center-of-mass energy of 500 GeV ILC

Shin-ichi Kawada

22/July/2016

Abstract

[1] This note is just a log of the analysis of $h \to \mu^+\mu^-$ mode at the 500 GeV ILC. This process is picked up as the one of the physics benchmark process of the ILD optimization, and try to measure its branching ratio.

As the first step, I performed an analysis using SGV samples, and also did an analysis using fully-simulated samples later. In this note I will describe both.

[1] Release note

- 2016/July/22 release
- 2016/July/29 modified, some typos are fixed
- 2016/August/2 just changed layout
- 2016/August/31 some typos are fixed
- 2016/September/13 modified, some numbers are fixed

1 Introduction

The ILD group is now working on ILD detector optimization. Of course if we want to measure all physics variables very precisely, it would be nice to build huge detector. However it leads us to pay huge amount of cost. The optimization process is to search the optimal size of detector, technologies, and so on by using the analysis results as the inputs.

We can try to optimize from various point of view, but in this note we will focus on the physics benchmark process. Table 1 shows the list of physics benchmark of the ILD. And we will discuss the analysis of $h \to \mu^+\mu^-$ channel.

Table 1: A list of ILD physics benchmark process [1]. JER (JES) means jet energy resolution (jet energy scale).

process	physics	detector performance	$\sqrt{s}$ (GeV)
$h \to cc$	BR	c-tag, JER	any
$h \to \mu\mu$	BR	high p tracking	500
$h \to \tau\tau$	BR, CP	τ reco., PID, track separation	250
$h \to bb$	M_h, BR	JES, JER, b-tag	500
$h \to$ invisible, $Z \to qq$	Higgs portal	JER	250
$e\nu W \to e\nu qq$	M_W, triple gauge coupling	JES, JER	500
$t\bar{t} \to 6$ jet	top coupling, A_{FB}	b-tag, jet charge	500
$\chi_1^+\chi_1^-$, $\chi_2^0\chi_1^0$, near degenerated	natural SUSY	low p tracking, PID	500
γXX	WIMPs	photon ES and ER, hermiticity	500

2 Cross section and number of events

A branching ratio of Higgs boson decaying into muon pairs is 2.2×10^{-4} [2]. By using the number of ILC cross section database [3] and the "H20" running scenario of the ILC which assumes an operating time of 20 years [4, 5], the expected number of signal events can be summarized as Table 2 and Table 3 (only for left/right-handed beam polarization case). In left-handed case, the most dominant process is $\nu\bar{\nu}h$, followed by $q\bar{q}h$. In right-handed case, the $q\bar{q}h$ process is dominant, however, the number of events less than 20.

Table 2: The expected number of events of $e^+e^- \to f\bar{f}h$ with $h \to \mu^+\mu^-$ process. We assumed the beam polarization of $P(e^-) = -0.8$ for electron, and $P(e^+) = +0.3$ for positron.

process	eL.pR	eR.pL	eL.pL	eR.pR	sum
$q\bar{q}h$	23.7	0.9	—	—	24.6
e^+e^-h	3.1	0.1	0.7	0.1	4.0
$\mu^+\mu^-h$	1.2	0.0	—	—	1.2
$\tau^+\tau^-h$	1.2	0.0	—	—	1.2
$\nu\bar{\nu}h$	59.8	0.3	—	—	60.1

Table 3: The expected number of events of $e^+e^- \to f\overline{f}h$ with $h \to \mu^+\mu^-$ process. We assumed the beam polarization of $P(e^-) = +0.8$ for electron, and $P(e^+) = -0.3$ for positron.

process	eL.pR	eR.pL	eL.pL	eR.pR	sum
$q\bar{q}h$	1.4	15.2	—	—	16.6
e^+e^-h	0.2	1.5	0.1	0.7	2.5
$\mu^+\mu^-h$	0.1	0.8	—	—	0.9
$\tau^+\tau^-h$	0.1	0.8	—	—	0.9
$\nu\bar{\nu}h$	3.6	4.5	—	—	8.1

3 Preparation of analysis

We will consider the process of $e^+e^- \to \nu\overline{\nu}h \to \nu\overline{\nu}\mu^+\mu^-$ with left-handed case as the signal because it has highest statistics. Before testing any kind of detector configurations, it would be good to consider the DBD configuration [6] as the staring point. The SM backgrounds which passed the full simulation under this configuration is already prepared. I used the samples under

`/pnfs/desy.de/ilc/prod/ilc/mc-dbd/ild/dst-merged/500-TDR_ws`

as the backgrounds (as of 2016/June). I included all of these samples, except 4f WW hadronic, ZZ hadronic, and 6f. The 4f hadronic processes produce many charged particles, and it would be easy to separate from the signal. I heard that some of the 6f samples are doubly produced. In order to avoid some double-counting, I did not include them. In future, I should include these if the problems are solved properly.

I confirmed that the existence of stdhep [7] files of $e^+e^- \to f\overline{f}h$ with $h \to \mu^+\mu^-$, but there were no slcio [8] files passed the full detector simulation. Therefore, we prepared the samples using SGV [9]. The SGV is a fast simulator, and this is not the tool of performing full detector simulation. But, it would be nice to use SGV if we want to test with various detector configurations, because we can save CPU time for producing enough number of samples. It takes huge amount of time when producing enough statistics sing full detector simulation.

After some time, the fully-simulated samples under the DBD configuration of signal process are prepared using ILCDirac [10]. The analysis using these will be discussed later.

4 Analysis using SGV samples

In this chapter we will discuss the analysis using SGV samples.

4.1 Event reconstruction

I required following 4 conditions for reconstructing muons. Next 4 figures are the distributions for each variable.

- $E_{\text{track}} > 15$ GeV
- $\dfrac{E_{\text{ECAL}}}{E_{\text{ECAL}} + E_{\text{HCAL}}} < 0.5$
- $\dfrac{E_{\text{ECAL}} + E_{\text{HCAL}}}{|P_{\text{track}}|} < 0.3$
- $\left|\dfrac{d_0}{\sigma(d_0)}\right| < 3$

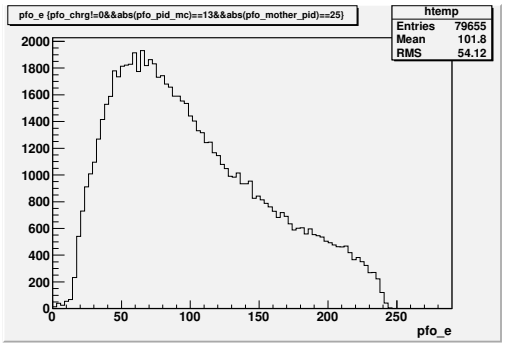

Figure 1: Distribution of $E_{\rm track}$.

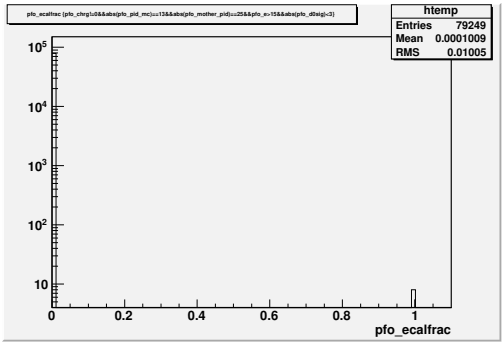

Figure 2: Distribution of $\dfrac{E_{\rm ECAL}}{E_{\rm ECAL}+E_{\rm HCAL}}$.

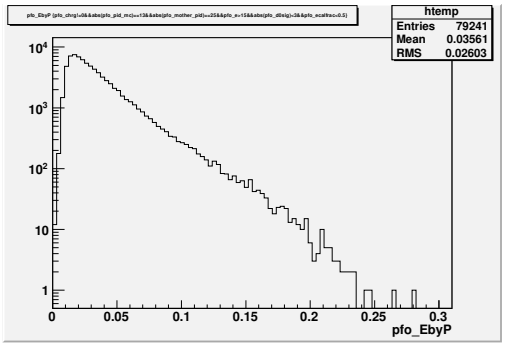

Figure 3: Distribution of $\dfrac{E_{\rm ECAL}+E_{\rm HCAL}}{|P_{\rm track}|}$.

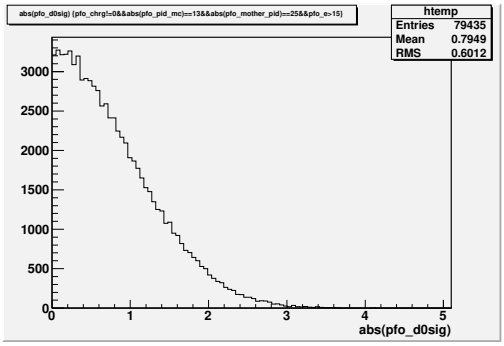

Figure 4: Distribution of $\left|\dfrac{d_0}{\sigma(d_0)}\right|$.

A reconstruction efficiency of 98.4% was obtained which exactly reconstruct one μ^+ and one μ^-. Of course we should not forget this is SGV sample.

After this reconstruction, I applied the correction to take care about FSR photons. The distribution of muon pair invariant mass goes to lower mass region due to FSR photons. The purpose of this correction is to correct FSR photon effect. The four-momentum of neutral particles which satisfy $\cos\theta > 0.99$ is added to reconstructed muon four-momentum, where θ is the momentum angle with respect to muon. The following 2 figures show the comparison of muon pair invariant mass with and without FSR correction (whole range and zoom up). Black histogram shows the distribution without FSR correction, while blue is the case with FSR correction under $\cos\theta > 0.99$ condition. It is clear that we have more events in corrected case.

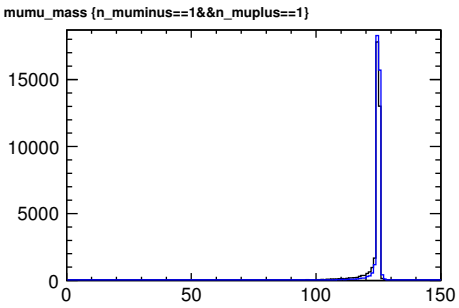

Figure 5: Distribution of muon pair invariant mass. The width of bin is 1 GeV / bin.

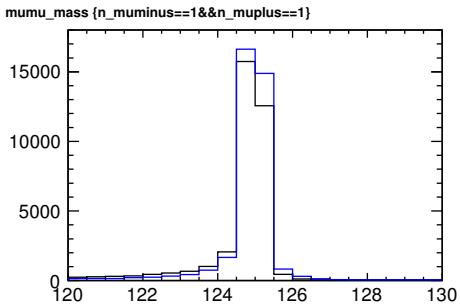

Figure 6: Distribution of muon pair invariant mass (zoom up). The width of bin is 0.5 GeV / bin.

4.2 Analysis

Before optimization I required following conditions as the precuts.

- events which have exactly one μ^+ and exactly one μ^-,
- number of tracks in an event should equal or less than 4,
- $124 < M_{\mu\mu} < 126$ GeV,

where $M_{\mu\mu}$ is reconstructed muon pair mass with FSR correction. The following 2 figures show the distribution of number of tracks and $M_{\mu\mu}$.

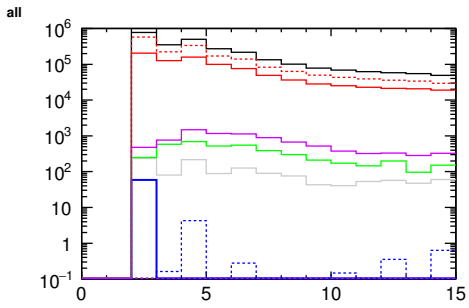

Figure 7: Distribution of number of tracks.

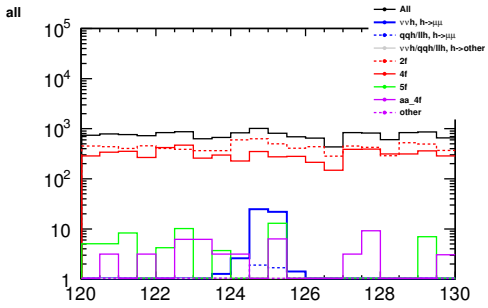

Figure 8: Distribution of muon pair invariant mass.

After that I applied these cuts as the optimum.

- visible $E_{\rm vis} < 285$ GeV,
- $P_t > 50$ GeV,
- thrust < 0.91,

where P_t is computed transverse momentum from the four-momentum of summing up of all visible particle's four-momentum. The following 3 figures shows the distribution of each variable.

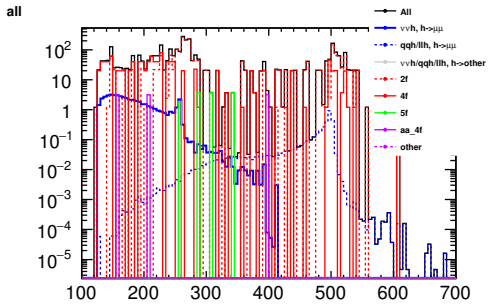

Figure 9: Distribution of E_{vis}.

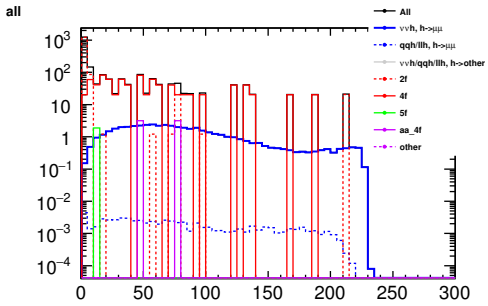

Figure 10: Distribution of P_t.

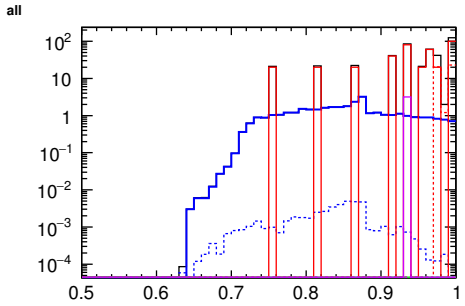

Figure 11: Distribution of thrust.

Table 4 shows the cut statistics of the analysis using SGV samples.

Table 4: A cut table of using SGV samples.

	$\nu\nu h$ $h \to \mu\mu$	qqh+$\ell\ell h$ $h \to \mu\mu$	ffh $h \to$ other	2f	4f	5f	$\gamma\gamma \to$ 4f
No cut	60.04	20.20	4.119×10^5	4.273×10^7	$3,802 \times 10^7$	2.208×10^5	3.356×10^5
# $\mu^{\pm}$	58.93	18.25	6669.55	1.998×10^6	1.125×10^6	5891.06	1.095×10^4
# tracks	58.93	4.47	528.13	1.135×10^6	4.901×10^5	1523.30	2725.73
$M_{\mu\mu}$	50.71	3.86	0	2135.56	1133.50	12.92	9.45
E_{vis}	50.19	0.08	0	1354.20	845.73	1.88	6.30
P_t	35.73	0.05	0	44.81	381.91	0	3.15
thrust	27.61	0.05	0	0	60.26	0	0

From the analysis I obtained $N_{\text{sig}} = 27.61$ and $N_{\text{bkg}} = 60.31$. Therefore, the statistical significance can be calculated as $\dfrac{27.61}{\sqrt{27.61 + 60.31}} = 2.94$, and the precision is $\dfrac{\Delta(\sigma \times \text{BR})}{(\sigma \times \text{BR})} = 34\%$.

5 Analysis using fully-simulated samples

In this section we will discuss the analysis using full simulation samples.

5.1 Event reconstruction

I required following 5 conditions to reconstruct muons. Next 5 figures show the distribution of each variable.

- $E_{\text{track}} > 15$ GeV
- $\dfrac{E_{\text{ECAL}}}{E_{\text{ECAL}} + E_{\text{HCAL}}} < 0.6$
- $\dfrac{E_{\text{ECAL}} + E_{\text{HCAL}}}{|P_{\text{track}}|} < 0.4$
- $E_{\text{yoke}} > 1$ GeV
- $\left|\dfrac{d_0}{\sigma(d_0)}\right| < 5$

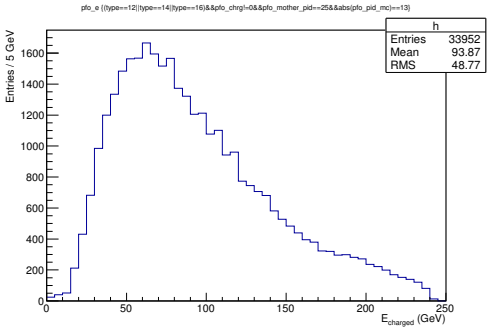

Figure 12: Distribution of E_{track}.

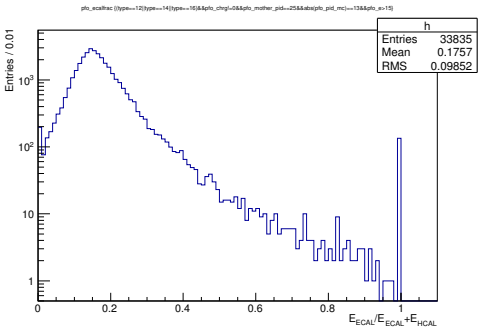

Figure 13: Distribution of $\dfrac{E_{\text{ECAL}}}{E_{\text{ECAL}} + E_{\text{HCAL}}}$.

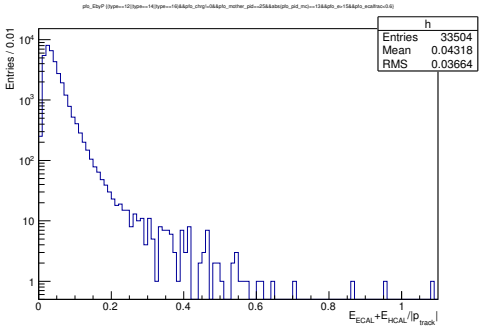

Figure 14: Distribution of $\dfrac{E_{\text{ECAL}} + E_{\text{HCAL}}}{|P_{\text{track}}|}$.

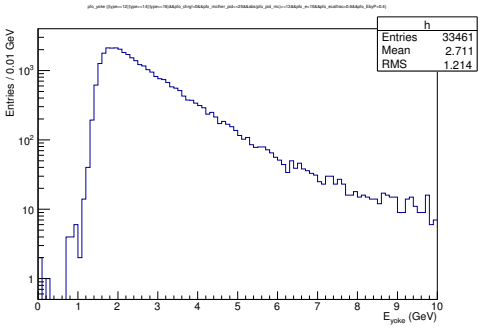

Figure 15: Distribution of E_{yoke}.

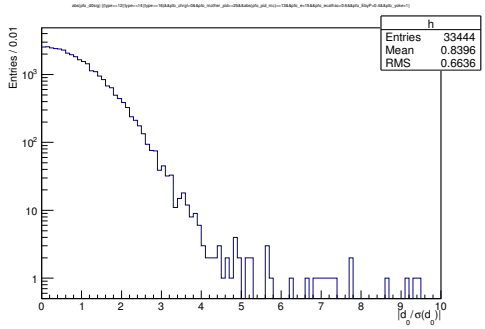

Figure 16: Distribution of $\left|\dfrac{d_0}{\sigma(d_0)}\right|$.

A reconstruction efficiency of 94.6% was obtained which exactly reconstruct one μ^+ and one μ^-.

After this reconstruction, I applied the correction to take care about FSR photons. The four-momentum of neutral particles which satisfy $\cos\theta > 0.99$ is added to reconstructed muon four-momentum, where θ is the momentum angle with respect to muon. The following 2 figures show the comparison of muon pair invariant mass with and without FSR correction (whole range and zoom up). Black histogram shows the distribution without FSR correction, while blue is the case with FSR correction under $\cos\theta > 0.99$ condition.

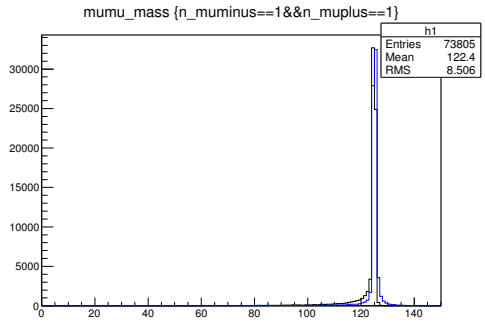

Figure 17: Distribution of muon pair invariant mass. The width of bin is 1 GeV / bin.

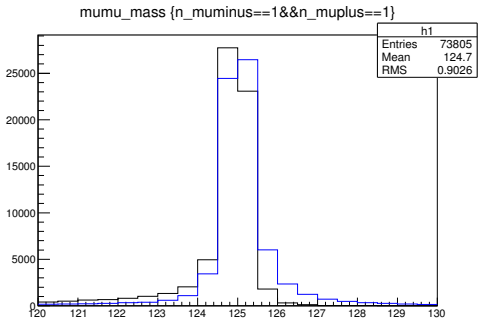

Figure 18: Distribution of muon pair invariant mass (zoom up). The width of bin is 0.5 GeV / bin.

5.2 Analysis

Before optimization I required the following conditions as the precuts.

- events exactly have one μ^+ and one μ^-,
- $N^{\rm track}_{E>15{\rm GeV}} \leq 4$,
- $124 < M_{\mu\mu} < 126$ GeV,

where $N^{\rm track}_{E>15{\rm GeV}}$ is the number of tracks which have energy greater than 15 GeV, and $M_{\mu\mu}$ is muon pair invariant mass with FSR correction. The reason why I required a cut to $N^{\rm track}_{E>15{\rm GeV}}$ is to avoid the effect of $\gamma\gamma \to$ hadron(s) overlay background. This background produces additional charged particles, therefore, the simple variable number of tracks is no longer useful to separate signal and background. However, the energy of $\gamma\gamma \to$ hadron(s) are tend to be low. In this situation, $N^{\rm track}_{E>15{\rm GeV}}$ would have some separation power. The following 2 figures show the distribution of $N^{\rm track}_{E>15{\rm GeV}}$ and $M_{\mu\mu}$.

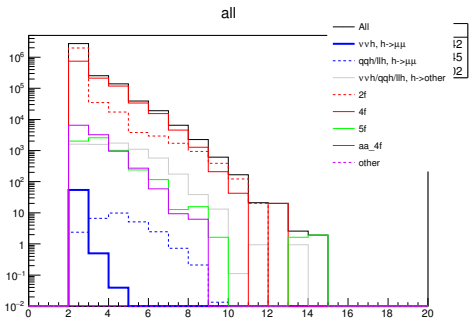

Figure 19: Distribution of $N^{\text{track}}_{E>15\text{GeV}}$.

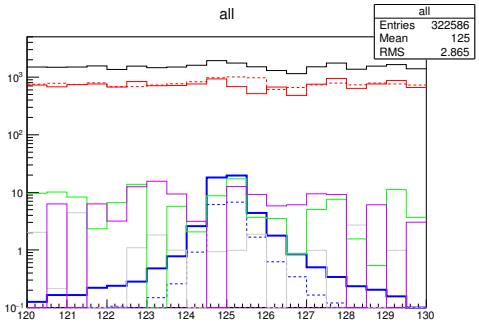

Figure 20: Distribution of muon pair invariant mass.

After that I applied following cuts as the optimum.

- visible energy $E_{\text{vis}} < 335$ GeV,
- $P_t > 25$ GeV,
- thrust < 0.91,
- $|\cos\theta_{\text{thrust}}| < 0.98$,
- $|\cos\theta_{\text{miss}}| < 0.98$,

where P_t is computed transverse momentum from the four-momentum of summing up of all visible particle's four-momentum, θ_{thrust} is the angle of thrust axis with respect to the beam axis, θ_{miss} is the missing angle with respect to the beam axis, respectively. The following 5 figures show the distribution of each variable.

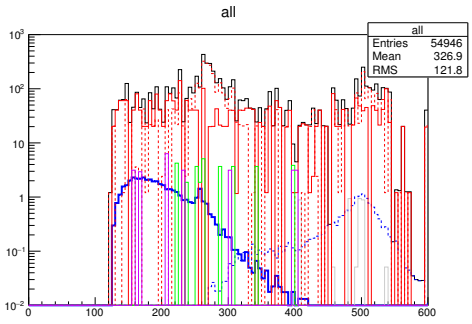

Figure 21: Distribution of E_{vis}.

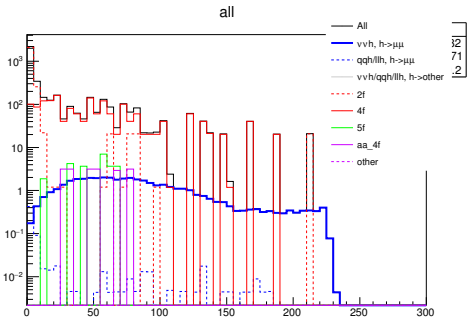

Figure 22: Distribution of P_t.

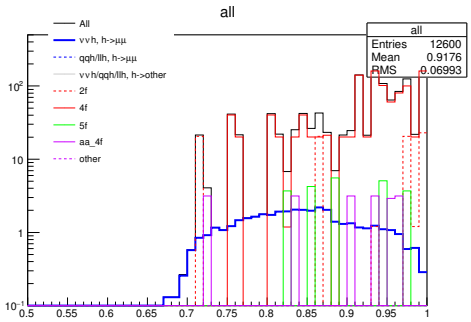

Figure 23: Distribution of thrust.

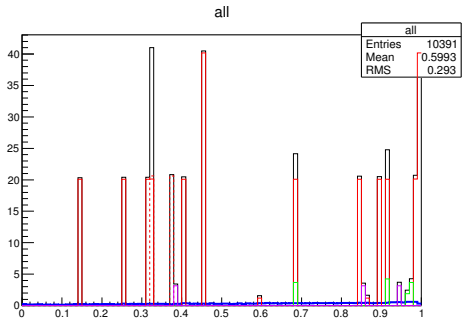

Figure 24: Distribution of $\cos\theta_{\text{thrust}}$.

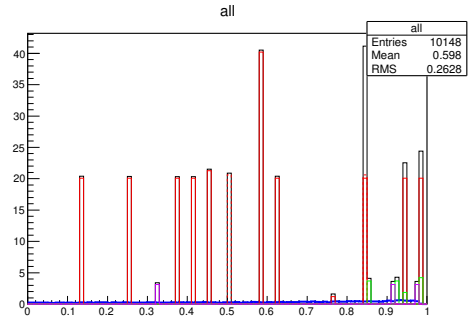

Figure 25: Distribution of $\cos\theta_{\text{miss}}$.

Table 5 shows the cut statistics using full simulation samples.

Table 5: A cut table using full simulation samples.

	$\nu\nu h$ $h\to\mu\mu$	qqh+$\ell\ell h$ $h\to\mu\mu$	ffh $h\to$ other	2f	4f	5f	$\gamma\gamma\to$ 4f
No cut	57.53	31.13	4.116×10^5	4.225×10^7	$3,808\times10^7$	2.209×10^5	3.356×10^5
# $\mu^\pm$	54.41	27.46	6818.81	2.025×10^6	1.124×10^6	5979.80	1.109×10^4
# $N^{\text{track}}_{E>15\text{GeV}}$	54.41	18.92	4920.84	2.015×10^6	1.069×10^6	5592.42	1.074×10^4
$M_{\mu\mu}$	44.70	15.46	3.80	3782.87	2894.26	31.63	24.96
E_{vis}	44.26	0.71	0	2454.88	1721.20	24.10	18.66
P_t	40.95	0.15	0	87.20	1129.30	22.22	18.66
thrust	32.88	0.15	0	41.19	283.65	13.46	9.45
$\lvert\cos\theta_{\text{thrust}}\rvert$	31.86	0.14	0	41.19	223.35	13.46	9.45
$\lvert\cos\theta_{\text{miss}}\rvert$	31.77	0.14	0	41.19	203.26	9.24	9.45

From the analysis, I obtained $N_{\text{sig}} = 31.77$ and $N_{\text{bkg}} = 263.28$. Therefore, the significance is $\dfrac{31.77}{\sqrt{31.77+263.28}} = 1.85$, and the precision is $\dfrac{\Delta(\sigma\times\text{BR})}{(\sigma\times\text{BR})} = 54\%$.

6 Summary and future plans

I evaluated $h\to\mu^+\mu^-$ channel at the center-of-mass energy of 500 GeV. This analysis is very challenging due to very small branching ratio. I performed analysis using SGV samples and fully-simulated samples both. I obtained the precision $\dfrac{\Delta(\sigma\times\text{BR})}{(\sigma\times\text{BR})}$ of 34% with SGV samples, and precision of 54% with full

simulation samples. The result of full simulation samples gave relatively $\sim 50\%$ worse than SGV case. One possible reason is the cut of number of tracks is not so useful, because it is strongly affected by $\gamma\gamma \to$ hadron(s) overlay background.

The future plan is as follows;

- introducing measurement error of muon pair mass including FSR correction $\sigma(M_{\mu^+\mu^-})$
- application of $\sigma(M_{\mu^+\mu^-})$: re-weighting
- further optimization using other variables, and introducing TMVA.
- separation of $e^+e^- \to Zh$ (Higgs-strahlung) and $e^+e^- \to \nu\overline{\nu}h$ (WW-fusion)

Unfortunately, we have limited number of background samples for the backgrounds now. We need to think about it if we move on to use TMVA.

References

[1] Junping Tian, Keisuke Fujii, Jenny List
"physics benchmarks for detector optimisation"
ILD Software & Optimization Workshop (2016/Feb./22-26)

[2] SM Higgs Branching Ratio and Total Decay Widths (update in CERN Report4 2016)
`https://twiki.cern.ch/twiki/bin/view/LHCPhysics/CERNYellowReportPageBR`

[3] `http://www-jlc.kek.jp/jlc/en/ilc-xsec-db`

[4] Keisuke Fujii, Christophe Grojean, Michael E. Peskin, Tim Barklow, Yuanning Gao, Shinya Kanemura, Hyungdo Kim, Jenny List, Mihoko Nojiri, Maxim Perelstein, Roman Pöschl, Jürgen Reuter, Frank Simon, Tomohiko Tanabe, Jaehoon Yu, James D. Wells, Hitoshi Murayama, Hitoshi Yamamoto
"Physics Case for the International Linear Collider"
arXiv:1506.05992v2 [hep-ex] (2015)

[5] T. Barklow, J. Brau, K. Fujii, J. Gao, J. List, N. Walker, K. Yokoya
"ILC Operating Scenarios"
arXiv:1506.07830v1 [hep-ex] (2015)

[6] Ties Behnke, James E. Brau, Philip Burrows, Juan Fuster, Michael Peskin, Marcel Stanitzki, Yasuhiro Sugimoto, Sakue Yamada, Hitoshi Yamamoto
"The International Linear Collider Technical Design Report Volume 4: Detectors"
arXiv:1306.6329 [hep-ex] (2013)

[7] Lynn Garren
"Stdhep 5.06.01Monte Carlo Standardization at FNAL Fortran and C Implmentation" (2006)
`http://cepa.fnal.gov/psm/stdhep/`

[8] F. Gaede, T. Behnke, N. Graf, T. Johnson
"LCIO — A persistency framework for linear collider simulation studies"
arXiv:physics/0306114 [physics.data-an] (2003), proceedings of CHEP03

[9] Mikael Berggren
"SGV 3.0 — a fast detector simulation"
arXiv:1203.0217 [physics.ins-det] (2012)

[10] `https://twiki.cern.ch/twiki/bin/view/CLIC/DiracUsage`